Constraining Quark and Gluon Momentum Fractions Accessed by Observables in Polarized pp Collisions at PHENIX and sPHENIX

Evan Croft[1] **and Christine Aidala**[1]

[1] *University of Michigan*

Observations of transverse single-spin asymmetries (TSSAs) in polarized proton-proton collisions at the Relativistic Heavy Ion Collider (RHIC) have proven useful for probing quark and gluon dynamics inside the proton. Such observations are made in 200 GeV proton-proton collisions in the Pioneering High Energy Nuclear Interaction Experiment (PHENIX) and the upcoming sPHENIX experiment at RHIC. Individual quarks and gluons, collectively known as partons, carry some fraction of the proton momentum, denoted x. Parton distribution functions (PDFs), at leading order, describe the probability of finding a given quark or gluon at a given x. Analyses of TSSAs for direct photon and open heavy-flavor hadron production, as well as open heavy-flavor decays, provide access to spin-dependent quark and gluon PDFs. A Monte Carlo study of these events is done using the PYTHIA event generator. After the appropriate kinematic cuts are applied, final state particles are traced back to their quark or gluon ancestors, and their respective momentum fractions are plotted. This procedure therefore tells us what range of momentum fractions and mix of partonic flavors can be accessed by each existing or planned measurement.

1. INTRODUCTION

This project began as a continuation of work done by Chris Platte in the summer of 2021; Chris ran PYTHIA simulations of proton collisions at RHIC energies and found the partonic momentum fractions accessed by pion production, a process used to constrain the tri-gluon correlation function, as described in Nicole Lewis' thesis [1]. Nicole also uses direct photon TSSAs as a clean probe of parton dynamics inside the proton, since direct photon production does not involve any fragmentation into final state hadrons [2]. Other analyses of open heavy-flavor (OHF) production and the semileptonic decays of OHF mesons are good probes of gluon dynamics [3] [4], and we aim to confirm this and, similar to direct photon events, constrain the momenta accessible by such analyses.

The first step in this project is to create a general framework within ROOT and TPythia (PYTHIA version 8.307 [5]) for performing these kinds of calculations. My implementation of this idea is a C++ class called pt_histos, which contains members for storing the histogram objects themselves, functions for filling histograms depending on final state transverse momentum, and a function for drawing and saving multipanel canvases that show these histograms. The pt_histos constructor takes in arguments that determine which partons will be plotted, which transverse momentum (p_T) bins will be used, and what name should be given to the saved file. The remainder of the work is in writing simulations that store the relevant information (i.e. final state p_T and partonic momentum fractions x) in a TTree such that the i^{th} entry in a branch of this tree corresponds to the i^{th} saved event. The analysis macros will then unpack the data from each entry in the tree and pass it to the member function of the pt_histos object. For both direct photons and open heavy flavor simulations, the PDF set used in PYTHIA is NNPDF 2.3 with quantum electrodynamics (QED) corrections [6], which is the default in PYTHIA 8.3 [5]. All simulations have the partonic transverse momentum (denoted pTHat by PYTHIA) constrained to a minimum of 4 GeV/c and a maximum of 16.5 GeV/c. These constraints are set using the PYTHIA flags pTHatMin and pTHatMax [5]. Simulations all use random seed 42. All analysis and simulation code can be found at https://github.com/largewedge/momentum-fraction-coverage.git .

t	Total (all partons)
u	up
d	down
a	anti-up
p	anti-down
g	gluons

Table S1. Parton labels used in the code string.

2. DIRECT PHOTONS

Beginning with direct photons seems natural, since we only need to do a few things, at least in principle: for any event generated by PYTHIA, check for any particles with PDG code 22. To further simplify our task, we instruct PYTHIA to only generate events that involve hard scattering processes that produce photons; this is done with a call to Pythia's ReadString function: pythia8->ReadString("PromptPhoton:all = on"). Apply the relevant kinematic cuts, specifically those for sPHENIX ($|\eta| < 1.1$), since they are broader than those for PHENIX ($|\eta| < 0.35$), and find the partons that participated in the hard scattering process for this event, then store their momentum fractions in a TTree. The PHENIX pseudorapidity cuts will be applied to the simulated data by the analysis macro if we wish to generate plots relevant to PHENIX instead of sPHENIX. It is important to note that for the i^{th} entry in any branch in this tree, the i^{th} entry of every other branch in the tree corresponds to the same event. Similarly, some of the branches will store vectors, since one event may contain more than one final-state particle of interest, although this is exceedingly rare for direct photon events. Then there are two indices we need to worry about, and it is the simulation macro's responsibility to ensure that in addition to the first index, which tells us which event a piece of data belongs to, the second index, j, refers to the same final-state particle for a given event i. For example, we would like to be able to make plots of momentum fractions accessed by photons according to which p_T bin they fall into, so we will create two branches for the scattering partons' momenta, two more for their PIDs, one that contains a vector of final-state photon momenta, and one that contains a vector of final-state photon energies, in case we are interested in using this information later for other purposes. Then, for any event that satisfies our kinematic cuts, the 2^{nd} entry in the vector of momenta corresponds to the same photon as the 2^{nd} entry in the vector of final-state energies, and so on for any number of entries.

For our analysis macro, we create a flag that indicates whether we are generating plots for PHENIX or sPHENIX. This determines the pseudorapidity cuts that will be applied, although the cuts will only be applied to PHENIX plots, since these will require the narrower of the two ranges. We also take as arguments to the macro a string that specifies the partons that will appear in the plot, and the name of the exported plot. The code-string for partons appears in the format "tudapg", where any character can be removed, and the characters are interpreted as in table S1.

Results relevant to the analysis presented in Ref. [2] are shown in Figs. S1 and S2. Results of the same procedure, but using pseudorapidity cuts appropriate for sPHENIX, are shown in Figs. S3 and S4.

The quarks clearly dominate in the valence region $x > 0.1$, while antiquarks do not contribute much to processes that result in direct photons. The direct photon TSSA from Ref. [2] is shown in Fig. S5.

Our results determine the range of momentum fractions that can be probed by this analysis, and therefore the domain over which these results can be said to constrain the twist-3 collinear correlation functions shown in the same plot.

3. OPEN HEAVY-FLAVOR

Other analyses of data from PHENIX focus on events that have final-state open heavy-flavor (OHF) hadrons, which are hadrons that contain one charm or bottom quark, but not the corresponding antiquark, or vice versa. The same type of analysis was done here as was done for direct photons; the only difference lies in the PDG codes used to select particles, and the settings passed to PYTHIA which are the strings "HardQCD: hardccbar = on" and "HardQCD: hardbbbar = on".

Fig. S1. Quark, gluon, and total momentum fraction distributions sampled by direct photon production in different p_T bins at PHENIX.

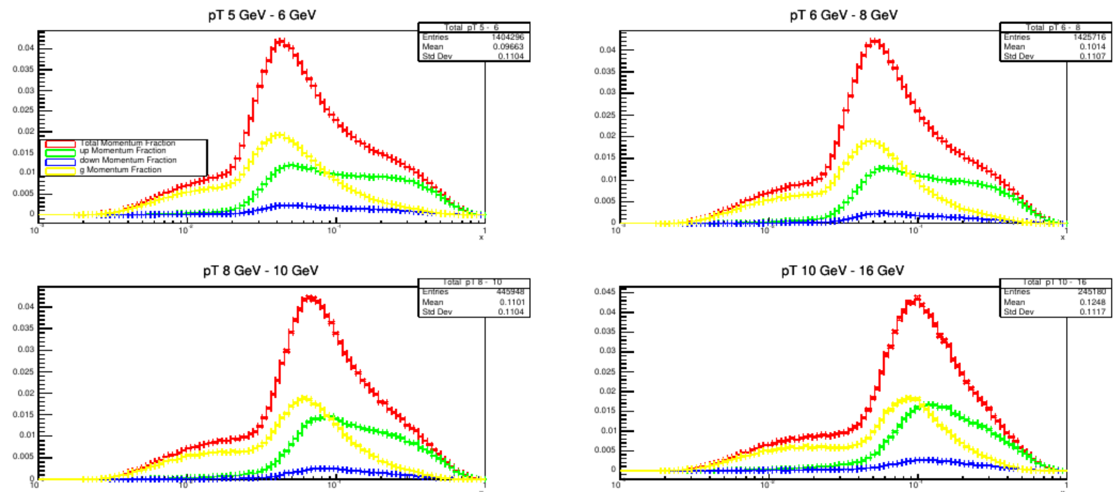

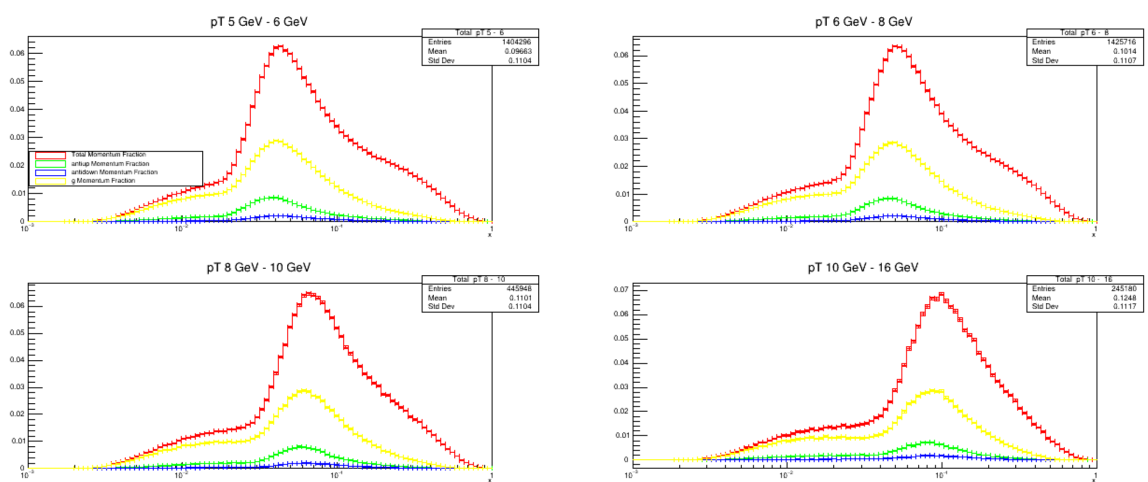

Fig. S2. Antiquark, gluon, and total momentum fraction distributions sampled by direct photon production in different p_T bins at PHENIX.

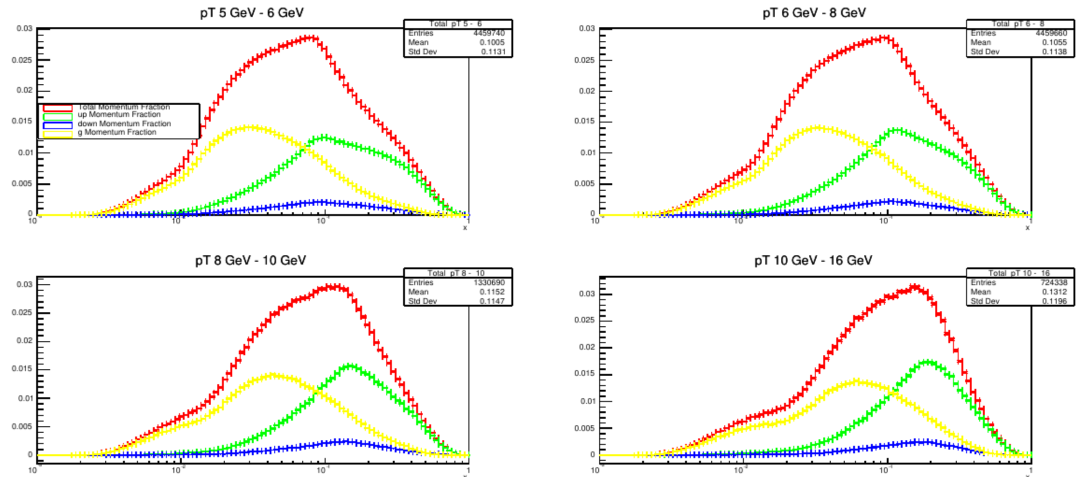

Fig. S3. Quark, gluon, and total momentum fraction distributions sampled by direct photon production in different p_T bins at sPHENIX.

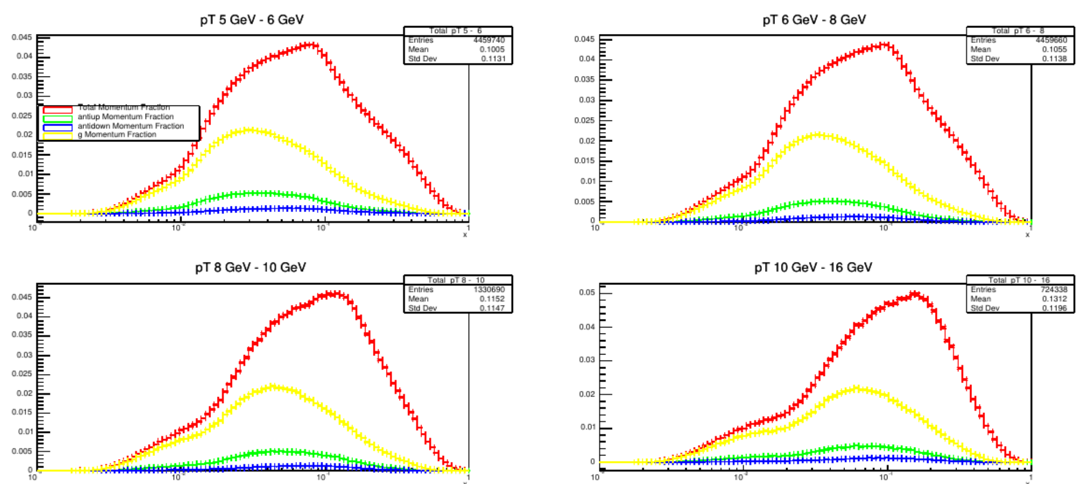

Fig. S4. Antiquark, gluon, and total momentum fraction distributions sampled by direct photon production in different p_T bins at sPHENIX.

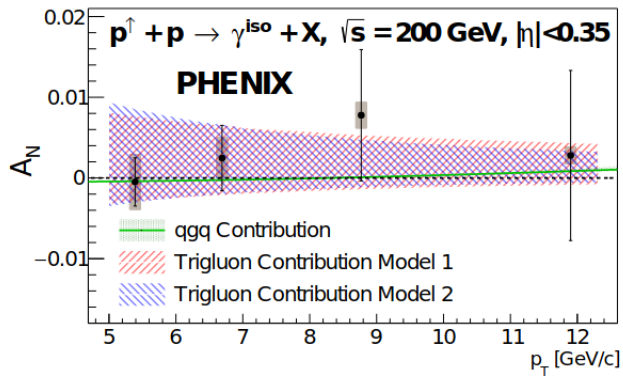

Fig. S5. The direct photon TSSA with theoretical predictions [2]

Light B-Meson PDG Codes	Light D-Meson PDG Codes
511	411
521	421
513	413
523	423
515	415
525	425
531	433
533	435
535	
541	
543	
545	

Table S2. PDG Codes used for selecting final state particles

PDG codes for selected final state particles in inclusive OHF production and the semileptonic decays discussed later are listed in table S2. Results from inclusive final-state OHF production are shown in Figs. S6 and S7.

These processes are clearly dominated by gluon dynamics inside the proton, as expected. Similarly, TSSAs for semileptonic OHF decays to electrons and muons are predicted to be dominated by gluon-gluon scattering. The pseudorapidity ranges for these analyses are different in addition to the underlying processes. Such plots are shown in Figs. S8 and S9.

Electrons are detected in the same pseudorapidity range as before, so the distribution of momentum fractions has not changed much. The relevant TSSA measurement is shown in Fig. S10.

Note the bimodal structure in Fig. S9. This is due to the geometry of the muon spectrometers in the PHENIX detectors, covering pseudorapidity ranges of $1.2 < \eta < 2.4$ and $-2.2 < \eta < 1.2$ for the north and south arms, respectively [4]. The TSSA for this decay channel is shown in Figs. S11 and S12 for positive and negative values of Feynman-x, $x_F = \frac{2p_z}{\sqrt{s}}$.

4. CONCLUSION

TSSAs are an invaluable tool for probing the inner structure of the proton, so it stands to reason that we will want to know in which regimes our measurements are relevant. This project has

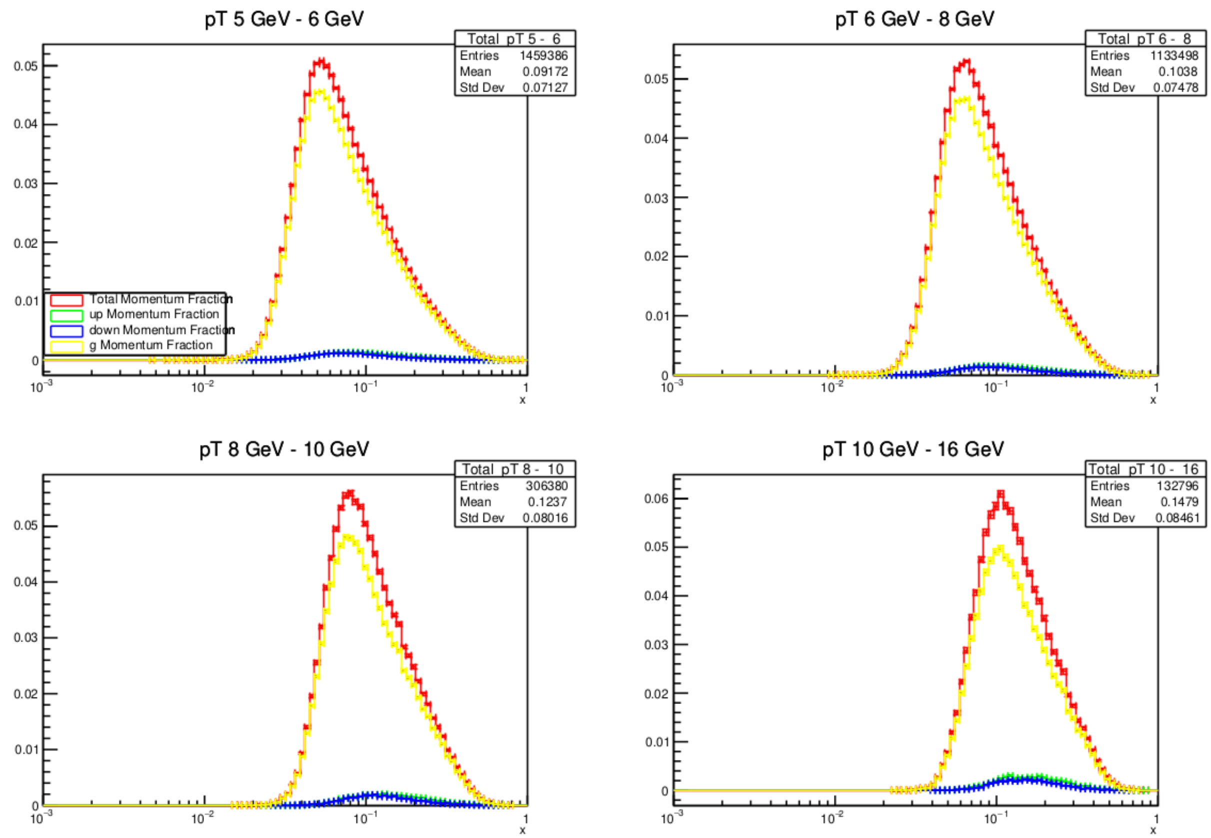

Fig. S6. Quark, gluon, and total momentum fraction distributions sampled by inclusive OHF production in different p_T bins at PHENIX

given us a way to constrain these measurements using only the geometry of the detector, the decay channel, and existing measurements of PDFs. Future continuations of this work would involve exploring more decay channels, namely for eta mesons and pions, and further exploring comparisons between the momentum fraction coverage offered by the upcoming sPHENIX experiment and that currently offered by PHENIX.

REFERENCES

1. N. Lewis, "Transverse Single-Spin Asymmetries of Midrapidity Direct Photons, Neutral Pions, and Eta Mesons in 200 GeV Polarized Proton-Proton Collisions at PHENIX," Other thesis, University of Michigan (2020).
2. U. A. Acharya *et al.*, "Probing Gluon Spin-Momentum Correlations in Transversely Polarized Protons through Midrapidity Isolated Direct Photons in $p^{\uparrow}+p$ Collisions at $\sqrt{s}$=200 GeV," Phys. Rev. Lett. **127**, 162001 (2021).
3. U. A. Acharya *et al.*, "Improving constraints on gluon spin-momentum correlations in transversely polarized protons via midrapidity open-heavy-flavor electrons in $p^{\uparrow}+p$ collisions at $\sqrt{s}=200$ GeV," (2022).
4. C. Aidala *et al.*, "Cross section and transverse single-spin asymmetry of muons from open heavy-flavor decays in polarized p+p collisions at $\sqrt{s}=200$ GeV," Phys. Rev. D **95**, 112001 (2017).
5. C. Bierlich *et al.*, "A comprehensive guide to the physics and usage of PYTHIA 8.3," (2022).
6. R. D. Ball, V. Bertone, S. Carrazza, L. Del Debbio, S. Forte, A. Guffanti, N. P. Hartland, and J. Rojo, "Parton distributions with QED corrections," Nucl. Phys. B **877**, 290–320 (2013).

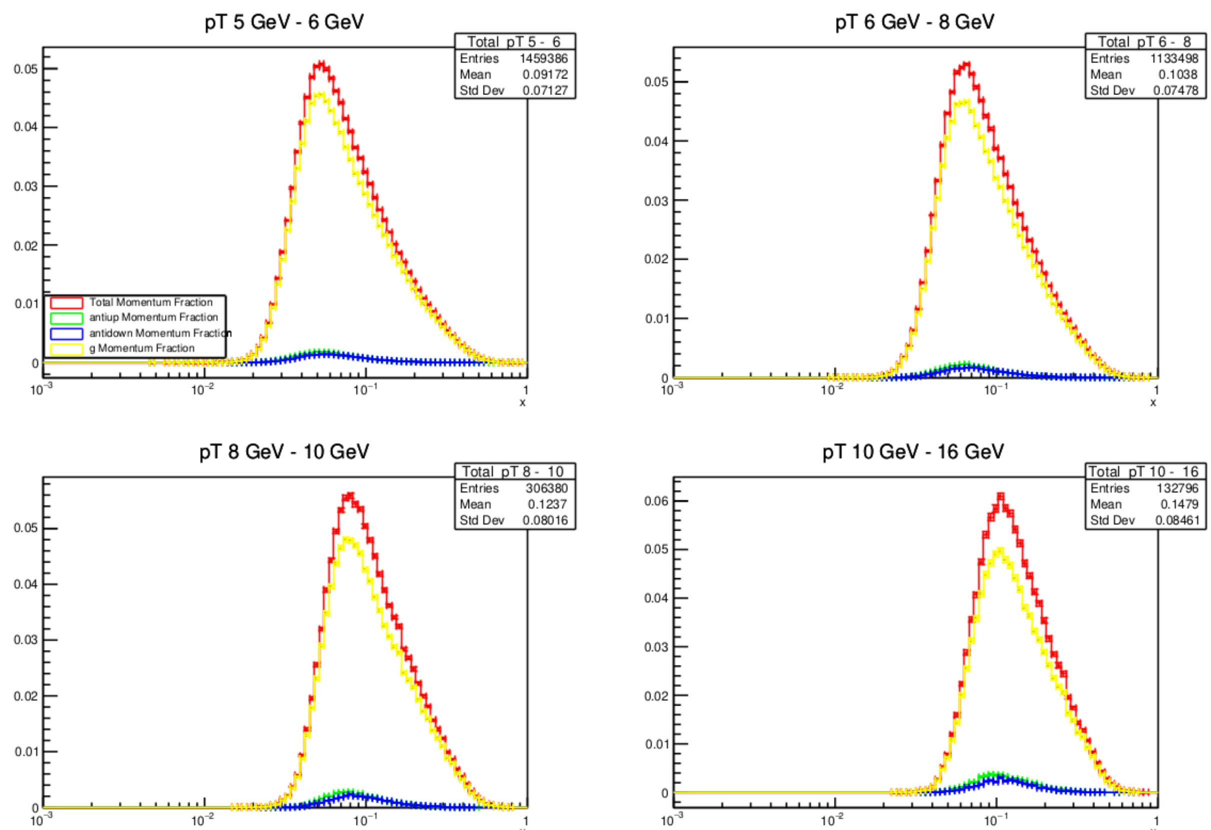

Fig. S7. Antiquark, gluon, and total momentum fraction distributions sampled by inclusive OHF production in different p_T bins at PHENIX

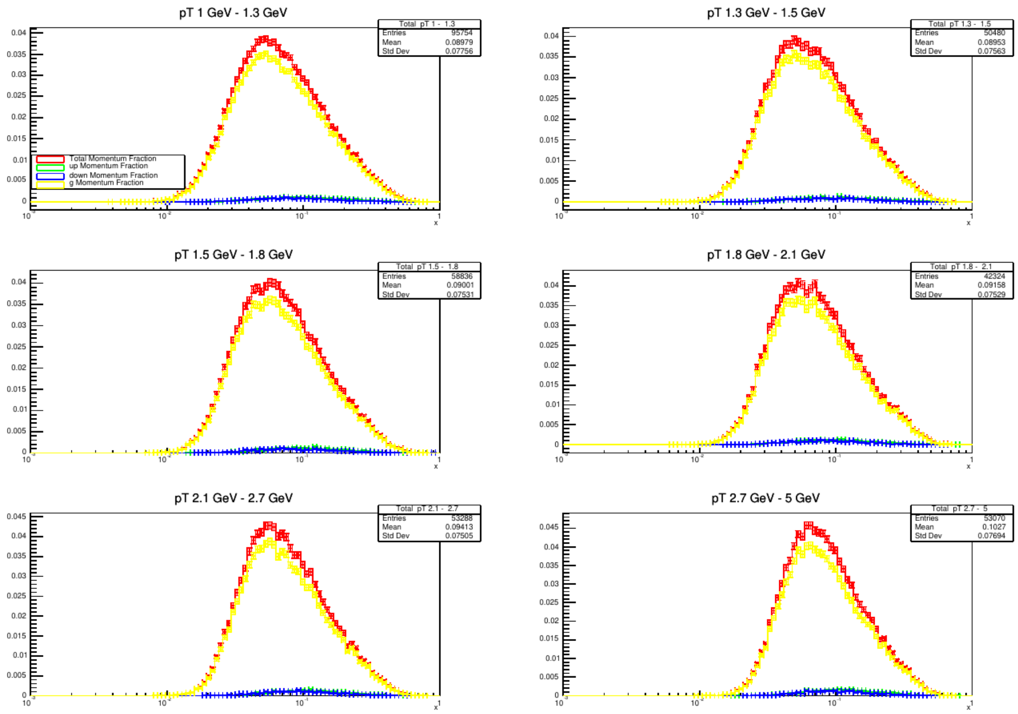

Fig. S8. Quark, gluon, and total momentum fraction distributions sampled by OHF→ $e^{\pm}$events at PHENIX

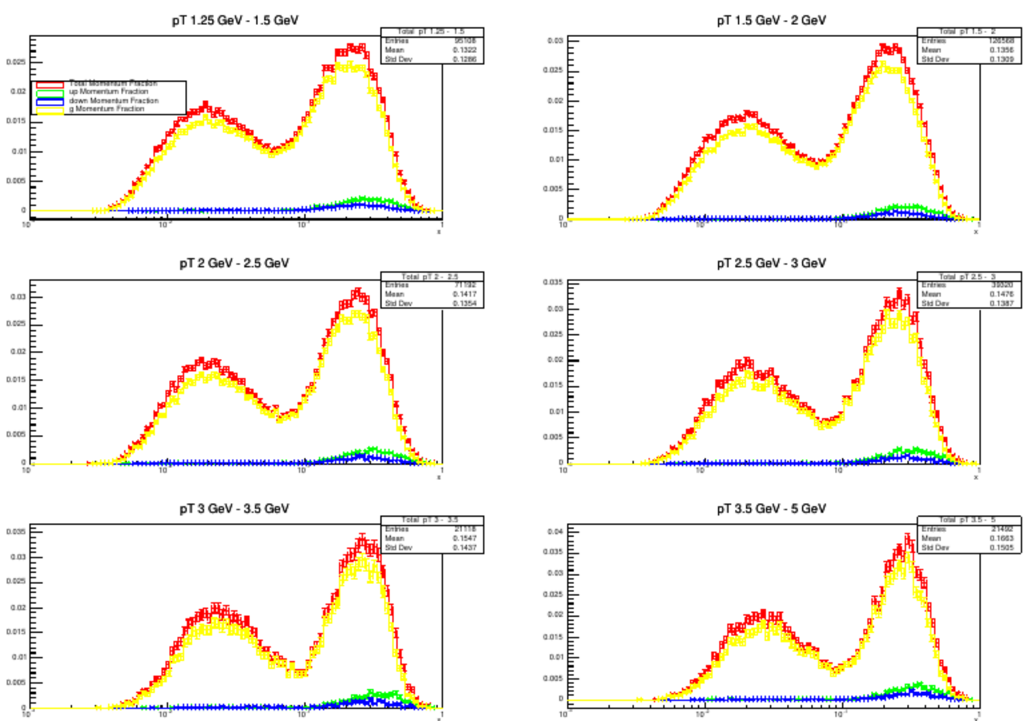

Fig. S9. Quark, gluon, and total momentum fraction distributions sampled by OHF→ $\mu^{\pm}$ events

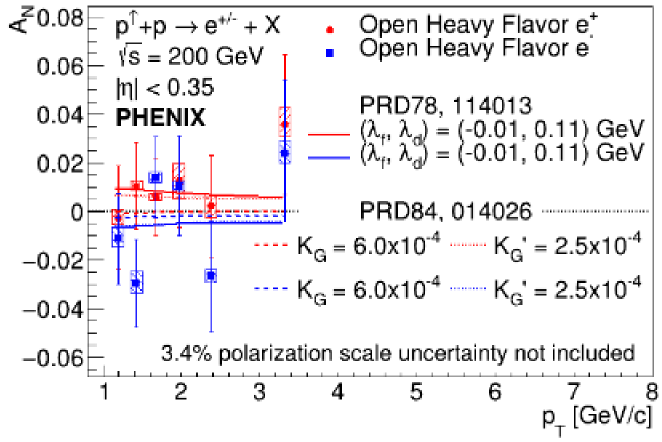

Fig. S10. OHF→ $e^{\pm}$ TSSA [3]

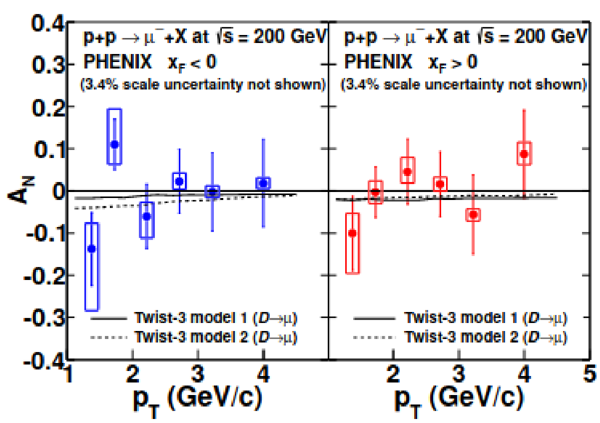

Fig. S11. OHF→ $\mu^{\pm}$ TSSA for $x_F > 0$ [4]

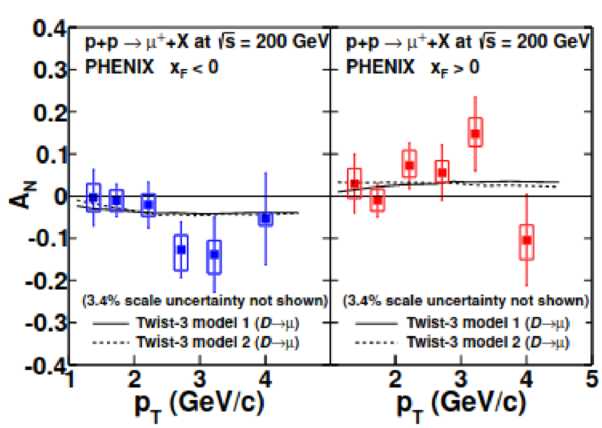

Fig. S12. OHF→ $\mu^{\pm}$ TSSA for $x_F < 0$ [4]